

## Boolean Dynamics of Kaufman Models with a Scale-Free Network

Kazumoto Iguchi

70-3 Shinhari, Hari, Anan, Tokushima 774-0003, Japan

Shuichi Kinoshita<sup>y</sup>Graduate School of Science and Technology, Niigata University,  
Ikarashi 2-Nochou 8050, Niigata 950-2181, JapanHiroaki S. Yamada<sup>z</sup>Yamada Physics Research Laboratory, 5-7-14 Aoyama, Niigata 950-2002, Japan  
(dated: January 12, 2022)

We study the Boolean dynamics of the "quenched" Kaufman models with a directed scale-free network, comparing with that of the original directed random Kaufman networks and that of the directed exponential-cut networks. We have numerically investigated the distributions of the state cycle lengths and its changes as the network size  $N$  and the average degree  $\langle k_i \rangle$  of nodes increase. In the relatively small network ( $N \leq 150$ ), the median, the mean value and the standard deviation grow exponentially with  $N$  in the directed scale-free and the directed exponential-cut networks with  $\langle k_i \rangle = 2$ , where the function forms of the distributions are given as an almost exponential. We have found that for the relatively large  $N \geq 10^3$  the growth of the median of the distribution over the attractor lengths asymptotically changes from algebraic type to exponential one as the average degree  $\langle k_i \rangle$  goes to  $\langle k_i \rangle = 2$ . The result supports an existence of the transition at  $\langle k_i \rangle_c = 2$  derived in the annealed model.

PACS numbers: 89.75.Hc, 05.40.-a

## I. INTRODUCTION

The origin of life has attracted many scientists as one of the unsolved problems in science for a long time [1]. To answer the quest, the self-organization of matter [2] and the emergence of order [3] have been regarded as the key ideas. Kaufman first introduced the so-called Kaufman model (a random Boolean network (RBN) model, based upon the random network theory [4, 5, 6]. This model has become a prototype for many authors to study complex systems such as metabolic stability and epigenesis, genetic regulatory networks, and transcriptional networks [3, 7, 8, 9, 10, 11, 12, 13] as well as general Boolean networks [14, 15, 16, 17, 18, 19], neural networks [20] and spin glasses [21, 22, 23].

In the RBN, we assume that the total number of the elements (i.e., nodes)  $N$  and the link number of an element (i.e., the degree of a node)  $K$  in a directed random network are kept to be constants, respectively. Kaufman found numerically that there is a phase transition from an ordered phase to a chaotic phase through the critical point (i.e., edge of chaos) at  $K = K_c = 2$  for the equally probable model of the Boolean functions for 0 and 1. Here in the chaotic phase the number of the state cycle attractors grows as exponential in  $N$ ; in the ordered phase the growth is proportional to  $N$ ; in the

critical point the growth is proportional to  $N^p$ . Later, this phenomenon has been analytically verified by studying the "annealed" Kaufman models [4, 15, 16]. And also exact results have been analytically obtained for the special cases of  $K = N$  [24, 25, 26, 27, 28, 29] and  $K = 1$  [30, 31, 32].

Recently there has appeared a revival interest on the study of the critical point of the Kaufman models with  $K_c = 2$  as well as  $K_c = 1$  where  $\langle k_i \rangle = 2p/(1-p)$  and  $p$  denotes a probability ( $0 < p < 1$ ) given in the next section [33, 34, 35, 36, 37, 38, 39, 40, 41, 42, 43]. Here, the power-law distributions of the cycle length of attractor [33], the models with the finite numbers of  $1 < K < 4$  [35, 36, 37], the special cases of  $K_c = 2$  networks such as the one-dimensional network and the Cayley tree [38], the scaling nature of the critical ( $K_c = 2$ ) point and the chaotic ( $K > 2$ ) phase [39], the superpolynomial growth of the number of the state cycle attractors [40], the stability of the system [41] have been studied both numerically and analytically. These results suggest that the critical point of Kaufman model with  $K_c = 2$  is very special.

Especially, Bastolla and Parisi [35, 36, 37] elucidated that what is important on the critical line is the effective connectivity  $K_{\text{eff}} < 1$  and that the critical point of the model exhibits the nature of percolation of information where the character shares much with that of  $K = 1$  studied by Flyvbjerg and Kjerfve [30]. To study this rather peculiar aspect further, Coppersmith et. al. [42, 43] studied numerically the "reversible" Kaufman model that is different from the original one in the sense that the former is dissipative while the latter is non-dissipative. They supplied a critical value of  $K_c = 1.62$  for the non-

<sup>E</sup>Electronic address: kazumoto@stannet.ne.jp<sup>y</sup>Electronic address: f01j06g@mail.cc.niigata-u.ac.jp<sup>z</sup>Electronic address: hyamada@uranus.dti.ne.jp

dissipative cases.

On the other hand, at nearly the end of 1990's the scale-free networks have been discovered from studying the growth of the internet geometry and topology [44, 45, 46, 50, 51]. After the discovery, scientists have become aware that many systems such as those which were originally studied by Kauffman as well as other various systems such as internet topology, human sexual relationship, scientific collaboration, economical network, and so on, belong to the category of the scale-free networks [44, 45, 46, 50, 51]. Therefore, it is very natural to apply the concepts of scale-free networks to the Kauffman model and to ask whether or not there appears the difference between the RBN and the scale-free random Boolean network (SFRBN).

Recently, as to this direction, the dynamics of the "quenched" SFRBN has been intensively studied [52, 53, 54, 55, 56, 58, 59, 60, 61, 62, 63]. It has been shown that the critical point occurs when the average degree  $\langle k_i \rangle$  of the scale-free networks equals  $\langle k_i \rangle_c = 2$  for the equal probability (i.e. no bias) models of  $p = 0.5$ , analytically studying the "annealed" SFRBN [52, 58, 59, 60] that are the scale-free analogs of the "annealed" RBN studied by Derrida and Pomeau [14]. Analytical results have been obtained for the annealed model with  $N \rightarrow \infty$  under some assumptions such as mean field approximation and ergodicity. On the other hand, a lot of numerical results have been calculated for finite-size quenched model. In the numerical simulation there are various ways for the sampling over, for example, (A) different networks, (B) different initial states, and (C) different Boolean functions assigned for each node. In particular, the mean value over the numerical distribution becomes insignificant when the distribution is broad because the order of fluctuation exceeds over the mean value. Then the relative fluctuation diverges for system size going to infinity, i.e. not self-averaging. Such a phenomena can be found at second-order phase transition and scale-free networks with power-law correlation [57]. In the situation the median value is statistically more robust against the artifacts due to undersampling of the set of the networks and the initial states than the mean value.

In this paper we would like to mainly investigate a qualitative transition in the function form of the median value  $m$  over the distribution of attractor length as a function of the finite  $N$ , changing the average degree  $\langle k_i \rangle$ . Note that the transition does not always mean phase transition in the usual statistical mechanics sense, which is defined in the thermodynamic limit of  $N \rightarrow \infty$ . One of our interests is also finite-size effect of the transition phenomena around  $\langle k_i \rangle = 2$  in the Boolean dynamics. How is the transition observed in the relatively small network corresponding to the realistic network size?

To ease the reference, we first summarize our main result: There is a transition of the function form  $m / N$  from  $< 1$  to  $> 1$  within a range of  $1.4 < \langle k_i \rangle_c < 1.7$  in the "quenched" SFRBN without bias. The transition becomes important when we consider some real-

istic biological networks, as Kauffman first introduced, because the realistic data suggest that the number of cell types in organism is crudely proportional to the linear or square-root function of the DNA content per cell,  $\propto N^{1/2}$  [1]. We adapted a completely synchronous updating rule in the Boolean dynamics because the attractor lengths are well-defined only for the synchronous updating rule. However, it is noting that the synchronism idealization is not always true for biological systems as genetic regulatory networks and asynchronous updating rules are more plausible for biological phenomena [64].

Moreover, the function form  $m(N)$  asymptotically changes from the algebraic type  $m(N) \propto 1/N$  to the exponential one as the average degree  $\langle k_i \rangle$  goes to  $\langle k_i \rangle = 2$ . This result is consistent with the previous belief that the transition occurs at the critical value of the degree of nodes of  $\langle k_i \rangle_c = 2$  in the "annealed" RBN and SFRBNs [3].

The organization of the paper is the following. In Sec. II, we present the Kauffman models that we study. In Sec. III, to apply various networks to the Kauffman models we give how to generate such networks. In Sec. IV, we study the cycle distributions of the "quenched" Kauffman models for the various network systems. In Sec. V, conclusions will be made. We mainly focused on the change of the functional form of the median around the critical value  $\langle k_i \rangle = 2$  in the main text. However, the other quantities such as Derrida plots and frozen nodes density are also used in order to investigate the Boolean dynamics. We briefly give analytical result for  $\langle k_i \rangle = 1$  in appendix A and Derrida plots in appendix B.

## II. RANDOM BOOLEAN NETWORK (RBN)

The RBN requires us to assume that the total number of nodes (vertices)  $N$  and the degree (the number of links) of the  $i$ -th node  $k_i$  are fixed in the problem, where all  $k_i = K$ . Since there are  $K$  inputs to each node,  $2^K$  Boolean functions can be defined on each node; the number  $2^K$  certainly becomes very large as  $K$  becomes a large number. Then, we assume that Boolean functions are randomly chosen on each node from the  $2^K$  possibilities. Locally this can be given by

$$x_i(t+1) = B_i(x_{i_1}(t); x_{i_2}(t); \dots; x_{i_K}(t)) \quad (1)$$

for  $i = 1; \dots; N$ , where  $x_i \in \mathbb{Z}_2 = \{0, 1\}$  is the binary state and  $B_i \in \mathbb{Z}_2$  is a Boolean function at the  $i$ th node, randomly chosen from  $2^{2^K}$  Boolean functions, where the probability to take 1 (or 0) is assumed to be  $p$  (or  $1-p$ ) (TABLE 1). In this paper we used a case of  $p = 1/2$  for the numerical calculations. But the treatment for other cases of  $p \neq 1/2$  is straightforward [65]. If we fix the set of the randomly chosen Boolean functions  $\{B_i; i = 1; \dots; N\}$  in the course of time development, then this model is called "quenched" model [7]. On the other hand, if we change each time the set of the

randomly chosen Boolean functions in the course of time development, then this model is called "annealed" model [14, 15, 16, 34].

$i_1$	$i_2$	$i_{k-1}$	$i_k$	$B_i$
0	0	0	0	1
0	0	0	1	2
0	0	1	0	3
0	0	1	1	4
$\vdots$	$\vdots$	$\vdots$	$\vdots$	$\vdots$
1	1	1	1	$2^{k-1}$

TABLE 1. The relationship between the Boolean functions  $B_i$  and inputs,  $f_{i_1}; i_2; \dots; i_{k-1}; i_k; g$ . Since there are  $k-1$ 's, each of which has 0 or 1, there are  $2^{k-1}$  ways of inputs. These provide  $2^{k-1}$ 's of outputs, each of which is 0 or 1, randomly chosen with a probability of  $p$  or  $1-p$ . Hence, there are possibly  $2^{2^{k-1}}$  Boolean functions at each node.

We then study the dynamics of the "quenched" RBN. Since there are  $N$  nodes in the random network, there are  $2^N$  states  $j = j_1; j_2; \dots; j_N$  in the system such as  $j = 0; 0; 0; \dots; 0; \dots; j_{2^N-1} = 1; 1; 1; \dots; 1$ . These states form all vertices of a hypercube in  $N$  dimensions. First, we start to define the initial state  $j^{(1)}$  out of the  $2^N$  states (for example, say  $j^{(1)} = 0; 1; 1; \dots; 0$ ). Second, according to the Boolean functions defined on the network, the initial state evolves to another state  $j^{(2)}$  in the  $2^N$  states. Hence, the time development can be simply denoted as

$$j^{(t+1)} = B_t j^{(t)}; \quad (2)$$

where each entry in  $j^{(t)}$  can be developed by Eq.(1) and  $B_t$  means a Boolean function chosen at time  $t$ . Therefore, if we collect all the  $2^N$  states as a  $2^N$ -dimensional vector  $j^{(t)} = (j; 0; 0; \dots; 0; \dots; j; 1; 1; \dots; 1)^T$ , then we can get a matrix representation of Eq.(2) as

$$j^{(t+1)} = \hat{B}_t j^{(t)}; \quad (3)$$

Here  $\hat{B}_t$  is a  $2^N \times 2^N$  matrix that all components are only 0 or 1, and  $j^{(t+1)}$  means a state vector whose components are degenerate such that the mapping of Eq.(3) is not a one-to-one but a many-to-one correspondence.

Considering this time developing equation, we find the cyclic structure of the states such as the length of the state cycle, the transient time and the basin size, and so on [3, 7, 19]. It is obviously difficult to do this procedure by an analytical method in general. Therefore, we must do it numerically [19] as well as analytically if possible. However, there are some important analytical results. The analytical investigations on the "annealed" models [14, 15, 16, 34] showed the existence of a phase transition at the critical value of  $K_c = 1/[2p(1-p)]$  [14, 15, 16, 34], and if we solve it conversely for  $p$  then

we obtain the critical value  $p_c = (1 - 1/(2K))^{1/2}$ . As is described in the introduction, the analytical methods for the systems with special values of the degree of nodes [24, 25, 26, 27, 28, 29, 30, 31, 40] have been studied in details, already.

### III. VARIOUS NETWORK MODELS

To apply the RBN to that with a given network, we have to specify what kind of network model we take. Since there are so many types of networks [46], we limit ourselves only to consider the directed random networks that were first considered by Kaufman [3], the directed scale-free networks, and the directed exponential-cut networks in this paper. But the generalization to other networks is straightforward. In this section, we will give how to generate such directed networks except the directed random networks, since the generation of those is very well known [4, 5, 6, 46, 47].

#### A. Directed scale-free networks with the integer average degree of nodes

Let us first consider the directed scale-free networks. In this case, we adopt a little modified version of the so-called Barabási-Albert model [45], since we have to treat the directed scale-free networks with fractional numbers of the average degree of a node (i.e., vertex),  $\langle k_i \rangle$ , such as  $1.5$  or  $2.1$ .

Denote by  $i$  the  $i$ -th node to which we want to put links and denote by  $j$  one of the surrounding nodes. Then, the input from the  $j$ -th node to the  $i$ -th node is described by the in-going arrow as  $i \leftarrow j$ , while the output from the  $i$ -th node to the  $j$ -th node is described by the out-going arrow as  $i \rightarrow j$ . Denote by  $k_i^{\text{in}}$  ( $k_j^{\text{in}}$ ) the input degree of the  $i$ -th node. Denote by  $k_i^{\text{out}}$  ( $k_j^{\text{out}}$ ) the output degree of the  $i$ -th node. We note that from simple consideration, when one input link to the  $i$ -th node is put between the  $i$ -th node and the  $j$ -th node, it becomes one output link for the  $j$ -th node at the same time. Therefore, if one input link is increased, so is one output link simultaneously.

Let us consider the case that the average degree of nodes,  $\langle k_i \rangle$ , is an even integer, such as  $\langle k_i \rangle = 2n$ . (A1) We initially start with  $m_0$  ( $n$ ) nodes for seeds of the system. We assume that both input and output links are simultaneously linked between all of the initial seed nodes. Therefore, the total link numbers for the input and the output are  $n(n-1)/2$  ( $n$ ), respectively. (A2) Next, every time when we add one node to the system,  $m = n - m_0$  new links are randomly chosen in the previously existing network, according to the preferential attachment probability for the output network,

$$i(k_i^{\text{out}}) = \frac{k_i^{\text{out}}}{\sum_{j=1}^{N(t)-1} k_j^{\text{out}}}; \quad (4)$$

(A 3) Similarly we redo the same procedure for the input network, according to the preferential attachment probability for the input network,

$$i(k_i^{\text{in}}) = \frac{k_i^{\text{in}}}{\sum_{j=1}^{N(t)-1} k_j^{\text{in}}} : \quad (5)$$

We continue the above procedures until the system size  $N$  is achieved. Therefore, after  $t$  steps, we obtain the total number of nodes as  $N(t) = m_0 + t$  and the total numbers of links for the input  $L^{\text{in}}(t)$  and output  $L^{\text{out}}(t)$  as  $L^{\text{in}}(t) = L^{\text{out}}(t) = L_0 + 2nt$ , respectively. Hence, by this we can obtain for the directed scale-free network  $h k_i^{\text{in}} i \sim 2L^{\text{in}}(t)/N(t) = 2n$ ,  $h k_i^{\text{out}} i \sim 2L^{\text{out}}(t)/N(t) = 2n$  as  $t \rightarrow \infty$ .

When  $h k_i = 2n + 1$ , after the procedure (A 3) we add one more procedure: (A 4) we redo the procedure (A 2) or (A 3) with equal probability.

#### B. Directed scale-free networks with the fractional average degree of nodes

Let us next consider the directed scale-free networks with a fractional average number of degree. Suppose that  $h k_i$  is fractional such that  $h k_i = [h k_i] + \{h k_i\}$  where  $[h k_i]$  means the integer part (say,  $n$ ) and  $\{h k_i\}$  the fractional part (say,  $f$ ) such that  $h k_i = n + f$ , where  $0 < f < 1$ .

In this case, (B 1) we first follow the same procedure (A 1) in the previous subsection A. (B 2) Second, we add one node to the system at each step of time. Every time when a new node is added, we have to define the node to give input or output. For this, we randomly choose input or output with equal probability of 0.5. (B 3) Third, if the chosen case is input (output) for the node, then we follow the procedure (A 2) [(A 3)] in the previous subsection A. Then, we place the input (output) links with equal probability 1 among the chosen links. (B 4) Fourth, if the not-chosen case is output (input) for the node, then we follow the procedure (A 3) [(A 2)] in the previous subsection A. Then, we place the output (input) links with equal probability  $f = n$  ( $0 < f < 1$ ) among the chosen links. (B 5) Fifth, go back to (B 2) and redo the same procedures until the system size  $N$  is achieved.

Then, after  $t$  steps, we obtain the total number of nodes  $N(t) = n + t$ , the total number of input links  $L^{\text{in}}(t) = L_0 + (n + f)t$ , and the total number of output links  $L^{\text{out}}(t) = L_0 + (n + f)t$ , respectively. Hence, we can obtain the average input and output degrees of nodes  $h k_i^{\text{in}} i \sim L^{\text{in}}(t)/N(t) = n + f$  and  $h k_i^{\text{out}} i \sim L^{\text{out}}(t)/N(t) = n + f$  as  $t \rightarrow \infty$ , respectively.

Using the above method, we can construct a scale-free network with a fractional average degree of nodes  $1 < h k_i < 2$ . For example, consider the case of  $h k_i = 1.4$ . In this case, we just take  $n = 1$  and  $f = 0.4$ .

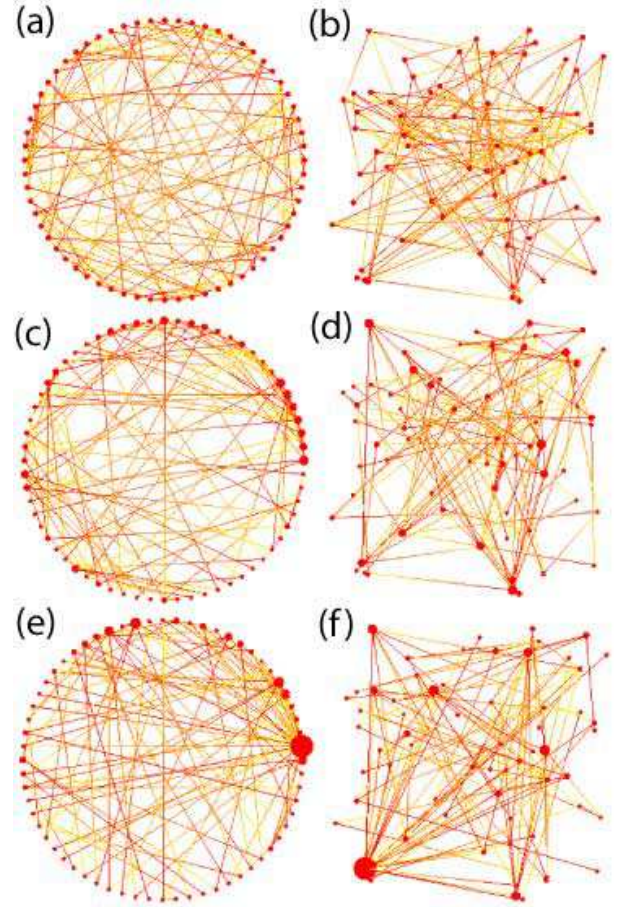


FIG. 1: (Color online) Typical examples of directed networks are shown for the size of  $N = 64$ . (a), (b) Random network with  $K = 2$ ; (c), (d) Exponential-attachment network with  $h k_i = 2$ ; (e), (f) Scale-free network with  $h k_i = 2$ . We show same network by two kinds of representation. For (a), (c) and (e) the nodes are located on the circumference with equal distance. For (b), (d) and (f) the nodes are randomly distributed in the square. Each node is represented as a bold point with size in proportion to the number of the input links. We represent input (output)-side of the links with deep (faint) color such that the direction of a link is denoted by the color gradation from deep color (output) to faint color (input).

#### C. Directed exponential-attachment networks

Let us consider the directed exponential-attachment networks. We can follow the same procedure for both the cases of the integer and fractional average degrees of nodes, replacing the probabilities of Eqs.(4) and (5) by

$$i(k_i^{\text{in}}) = i(k_i^{\text{out}}) = \frac{1}{m_0 + t} : \quad (6)$$

The exponential-like distributions are often observed in some real-world networks [48]. The generalization to other networks can be straightforward [49].

Fig.1 shows typical examples of the directed networks

where the total number of nodes  $N = 64$  is used: (a),(b) the directed random network with the degree of nodes,  $K = 2$ ; (c),(d) the directed scale-free network with the average degree of nodes,  $\langle k_i \rangle = 2$ ; and (e),(f) the directed exponential-uctuation networks with the average degree of nodes,  $\langle k_i \rangle = 2$ , respectively.

#### IV. CYCLE DISTRIBUTIONS

Now we are going to apply the above-mentioned "quenched" Kau man's Boolean dynamics to the directed random networks, the directed scale-free networks, and the directed exponential-uctuation networks. The first one provides the famous "quenched" RBN, the second one the "quenched" SFRBN model, and the third one the "quenched" exponential-uctuation random boolean network (EFRBN) model[3].

Before going to present the numerical results, let us explain the calculation method for obtaining the lengths of the state cycles as follows: (i) Realizations: We first prepare 1;000 sample networks with the size of  $N$  and investigate them in order. (ii) Initial conditions: Second, we randomly choose an initial state  $j^{(0)}$  out of the  $2^N$  states. (iii) The "quenched" Boolean dynamics: Third, we calculate the "Boolean dynamics" [given by Eq.(2)] repeatedly from 10 times to 100;000 times, where we use a special set of the Boolean functions on the network. This means that we treat the "quenched" model. (iv) State cycles: Fourth, we investigate whether there exist the states that belong to the equivalent state in the data. Since the "Boolean dynamics" is deterministic, if the state  $j^{(t_1)}$  at time  $t = t_1$  is the same as the state  $j^{(t_1+s)}$  at  $t = t_1 + s$ , then the state  $j^{(t_1+1)}$  at  $t = t_1 + 1$  becomes the same state as the state  $j^{(t_1+s+1)}$  at time  $t = t_1 + s + 1$ . Therefore, the length of the state cycles satisfying this condition is  $s + 1$ . Such calculations are performed for all network samples.

##### A. Histograms of the lengths $\ell_c$ of the state cycles

Fig 2 shows the histogram of the lengths  $\ell_c$  of the state cycles in the original "quenched" RBN with  $K = 2;4$  and in the "quenched" SFRBN and EFRBN where the average degree of nodes  $\langle k_i \rangle = 2;4$ . We can see that the functional forms of the distributions seem exponential type. The tail of the distribution depends on the fluctuation property of the degree of the nodes. We found that in comparing among the three types of the network structures the maximum length of the state cycle becomes longer as the fluctuation in the degrees of nodes becomes larger. We try to investigate them more accurate functional form of the distribution and the transition depending on the degree of nodes  $K$  and  $\langle k_i \rangle$ .

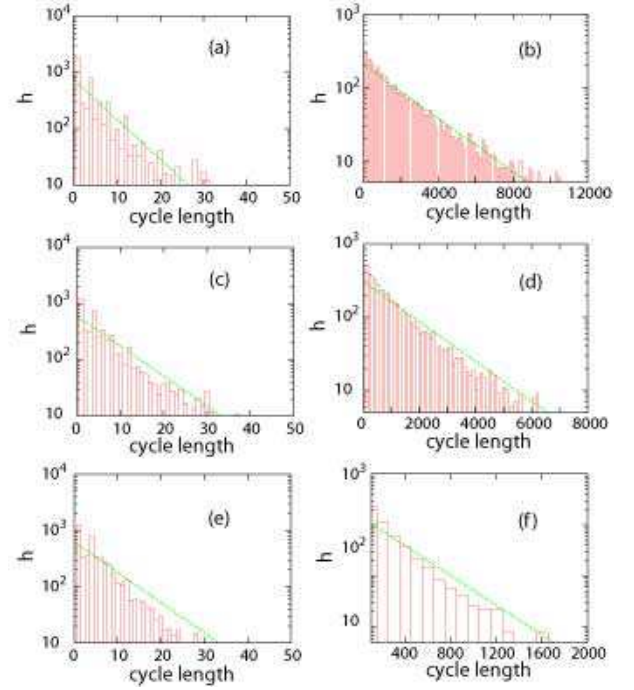


FIG. 2: (Color online) Histograms of the lengths  $\ell_c$  of state cycles in various types of the directed networks. The network size is  $N = 40$ . Each histogram is generated by  $10^3$  different sets of the Boolean functions and five different network structures. The maximum iteration number of the Boolean dynamics is  $10^5$  until the convergence to the cycle is realized. (a)-(b) RBN with  $K = 2;4$ ; (c)-(d) EFRBN with  $\langle k_i \rangle = 2;4$ ; (e)-(f) SFRBN with  $\langle k_i \rangle = 2;4$ . Here in (a)-(b)  $2^{2^K}$  Boolean functions of  $K$  variables are used equiprobably, while in (c)-(f)  $2^{2^{k_i}}$  Boolean functions of  $k_i$  variables are used equiprobably at the  $i$ -th node. The lines are the exponential fittings to the numerical data. The mesh sizes of the histograms are 1 for  $K = 2$  and  $\langle k_i \rangle = 2, 10^2$  for  $K = 4$  and  $\langle k_i \rangle = 4$ .

B. The median  $m$ , the mean value  $\langle \ell_c \rangle$ , and the standard deviation of the distributions of the state cycle lengths

Fig 3 shows the median  $m$ , the mean value  $\langle \ell_c \rangle$ , and the standard deviation of the distributions of the state cycle lengths with respect to the total number  $N$  ( $150$ ) of nodes for the various directed networks, respectively. Fig. 3(a) shows that in the RBN with  $K = 2$  the median grows as  $\sqrt{N}$  in relatively small  $N$  region and it grows as proportional to  $N$  in the large  $N$ . Whether or not the behavior of  $\sqrt{N}$  is valid is very delicate since we have to always stem this from the numerical data of the finite size systems. The more details will be shown elsewhere [65].

On the other hand, in the RBN with  $K = 4$  the median grows exponentially with  $N$  as  $m \sim e^N$ . We have observed that as  $K$  increases, the growth type of the median exhibits a transition from algebraic type to exponential one in the RBN. In the EFRBN and the SFRBN, the median grows exponentially with  $N$  for  $\langle k_i \rangle = 2$  and 4,



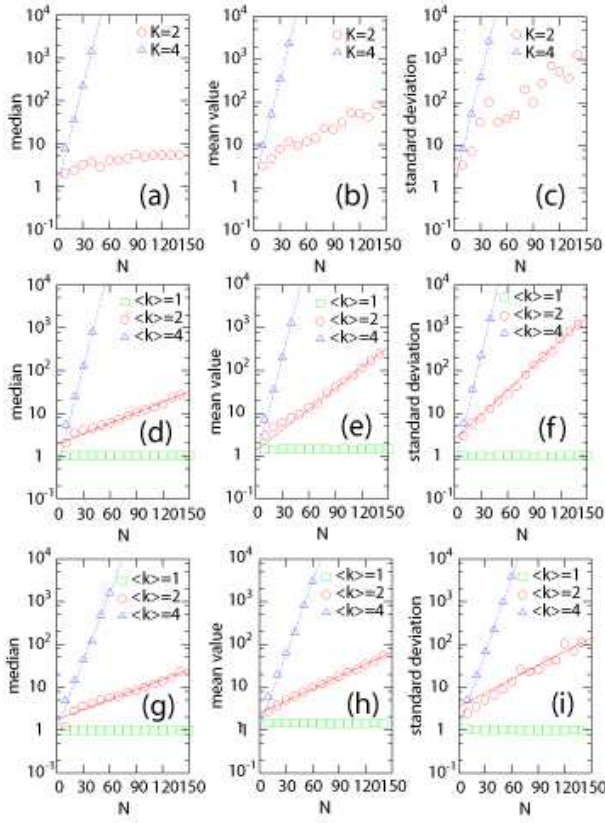


FIG. 3: (Color online) Semi-log-plots of the median  $m$ , the mean value  $h'_c$ , and the standard deviation  $\sigma$  of 5000 samples of the state cycles with respect to the total number  $N$  of nodes for the various directed networks, respectively. (a)-(c) are shown for the RBN with  $K = 2;4$ . (d)-(f) are shown for the EFRBN with  $h_{ki} = 1;2;4$ . And (g)-(i) are shown for the SFRBN with  $h_{ki} = 1;2;4$ . The lines are best exponential fittings,  $m \sim e^{aN}$ ,  $h'_c \sim e^{bN}$ ,  $\sigma \sim e^{cN}$ , to the numerical data except for the RBN with  $K = 2$ . The best fitted exponents are  $a = 0.02; b = 0.037; c = 0.044$  for the EFRBN with  $h_{ki} = 2$ ;  $a = 0.0168; b = 0.022; c = 0.025$  for the SFRBN with  $h_{ki} = 2$ ;  $a = 0.163; b = 0.193; c = 0.194$  for the RBN with  $K = 4$ ;  $a = 0.170; b = 0.179; c = 0.194$  for the EFRBN with  $h_{ki} = 4$ ;  $a = 0.123; b = 0.131; c = 0.136$  for the SFRBN with  $h_{ki} = 4$ .

and such a transition can not be observed in the range between  $h_{ki} = 2$  and  $h_{ki} = 4$ . Therefore, we conjecture that based on Fig.3, the transition takes place in the range between  $h_{ki} = 1$  and  $h_{ki} = 2$  in the RBN and the EFRBN. Note that  $N$  dependence for  $h_{ki} = 1$  can be analytically derived. (See appendix A.)

Furthermore, we can see the mean value  $h'_c$  and the standard deviation  $\sigma$  grow exponentially with  $N$  such as  $h'_c \sim e^{bN}$ ,  $\sigma \sim e^{cN}$ , in all cases. It is difficult to distinguish clearly the dynamical properties between the SFRBN and the EFRBN when the network size  $N$  is as small as  $N = 150$ .

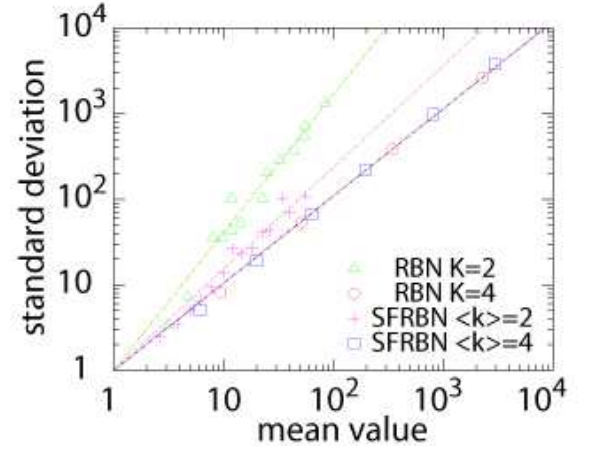


FIG. 4: (Color online) The relationship between the mean value  $h'_c$  and the standard deviation  $\sigma$  of the distributions of the state cycle lengths with respect to the total number  $N$  of nodes for the RBN with  $K = 2;4$  and the SFRBN  $h_{ki} = 2;4$ , respectively. The lines are fitting to the numerical data as  $\sigma = h'_c$ . The best fitted exponents are  $\alpha = 1.61; 1.02$  for the RBN with  $K = 2;4$ , and  $\alpha = 1.19; 1.02$  for the SFRBN with  $h_{ki} = 2;4$ , respectively. The result for the EFRBN is almost the same as that for the SFRBN.

C. The relationship between the mean value  $h'_c$  and the standard deviation

Fig.4 shows the relationship between the mean value  $h'_c$  and the standard deviation  $\sigma$  of the distributions of the lengths of the state cycles with respect to the total number  $N$  of nodes for the RBN and the SFRBN, respectively. We have found that the relationship is fitted by the following expression:  $\sigma = h'_c$ . The best fitted exponent  $\alpha$  is nearly equal to unity for  $K = 4$  and  $h_{ki} = 4$ . As a matter of fact, we can guess that in the continuum limit of the relatively large  $N$ , the distribution  $P(\ell_c)$  approaches the exponential form  $P(\ell_c) = \exp(-\ell_c)$ , as  $K$  and  $h_{ki}$  increases. In the exponential distribution, the mean value  $h'_c$  and the standard deviation  $\sigma$  can be represented in terms of the single parameter  $\lambda$  such as  $h'_c = 1/\lambda$ ,  $\sigma = 1/\lambda$ .

D. Plots of the median value  $m$

As shown in Fig.4 it is clear that the standard deviation  $\sigma$  is larger than the mean value  $h'_c$  for  $K = 2$  and  $h_{ki} = 2$ . In these cases, the numerical mean values are sometimes without credibility due to the lack of the samples with large cycle lengths. Such an imperfection of the self-averaging is well-observed for the distributions with a long-tail. Therefore, we investigate the relatively stable median as representative values to characterize the distributions of the attractor lengths, instead of the mean, for the large networks.

Fig.5 shows the median value  $m$  of the distribution of

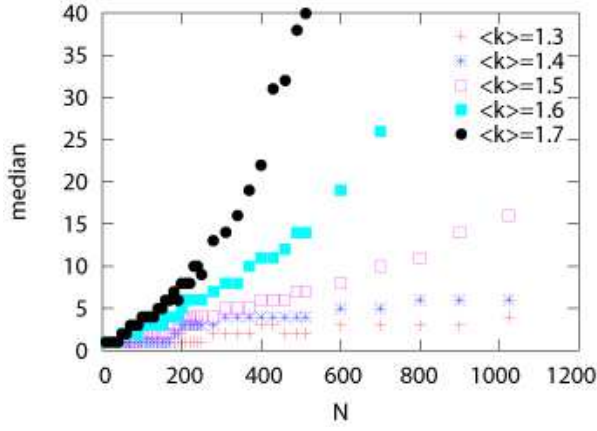


FIG. 5: (Color online) Plots of the median value  $m$  of 1000 samples of the lengths of the state cycles with respect to the total number  $N$  of nodes for the directed scale-free networks with  $\langle k \rangle = 1.3, 1.4, 1.5, 1.6$  and  $1.7$ . The results for  $N$  up to 1024 are shown. We used a cut-off attractor cycle length  $l_{\text{cut}} = 10^5$  due to the numerical difficulty to detect the large cycle length. For the 10-20 network samples, we did not detect the attractor cycle lengths. However, it seriously does not influence on the median of the distribution.

state cycle lengths with respect to the total number  $N$  of nodes for the relatively large SFRBN ( $N \sim 10^3$ ). We found that there is a transition in a range of  $1.4 < \langle k \rangle_c < 1.7$ , dividing the  $N$  ( $< 1$ ) growth and  $N$  ( $> 1$ ) growth in polynomial growth in the ordered phase. Note that some biological data suggest slow growth as  $N$  ( $< 1$ ) in the relatively small network size ( $N \sim 10^3$ ).

It is well-known that the scale-free topologies are ubiquitously in nature and the degree exponents lie in between 2 and 3. Furthermore, one of the important property in the scale-free topology is the existence of the highly connected hub as seen in the yeast synthetic network and so on [66]. The realistic systems do not contain enough nodes to closely approximate the true transition, therefore, the finite-size behavior is important. In fact some biological realistic data suggest that the number of cell types in organism is crudely proportional to the linear or square-root function of the DNA content per cell, i.e.  $m/N$  ( $< 1$ ) [3], for the finite-size  $N \sim 10^3$ .

Finally, we investigate a transition between the polynomial growth in the ordered phase and the exponential one in the chaotic phase. Figure 6 shows the semi-log and log-log plots of the data near  $\langle k \rangle_c \sim 2$  in Fig. 5. It is suggested that the function form  $m(N)$  has an polynomial form for  $\langle k \rangle < 2$  and approaches the exponential form as  $\langle k \rangle \rightarrow 2$  in the quenched SFRBN. The results are consistent with the critical value  $K_c = 2$  given for annealed SFRBN in other reports [52, 58, 59, 60]. In this section we focused on the scaling of attractor length near critical value  $\langle k \rangle \sim 2$ . The other quantities are also useful measure for the transition of the Boolean dynamics. (See appendix B.)

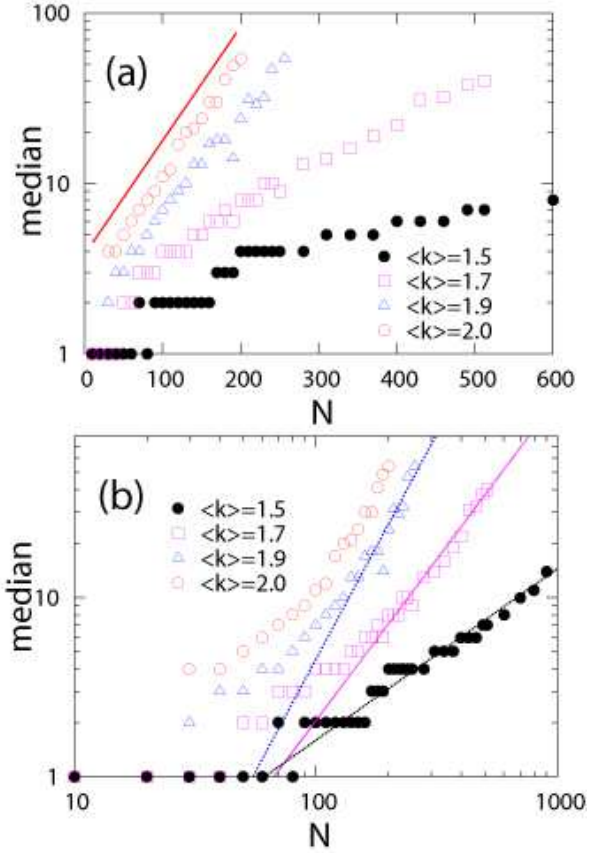


FIG. 6: (Color online) (a) Semi-log-plots and (b) log-log-plots of the median  $m$  with respect to the total number of nodes for some values  $\langle k \rangle$  near  $\langle k \rangle_c = 2$  for the scale-free network in Fig. 5. Apparently, the case with  $\langle k \rangle = 2$  exponentially increases with respect to  $N$ . The straight line in (a) shows the exponential growth for a guide for eyes, and the straight lines in (b) show the polynomial growth ( $m/N$ ) with the slopes  $= 2.5; 1.8; 0.98$  from top to bottom.

## V. CONCLUSIONS

In conclusion, we have studied the Boolean dynamics of the "quenched" Kauffman model with directed scale-free networks (SFRBN), comparing with ones of the directed random networks (RBN) and the directed exponential-uctuation networks (EFRBN). We have numerically calculated the distributions of the lengths of the cycles and its changes as the network size  $N$  and the average degree of the node increase. We have found that the median, the mean value and the standard deviation grows exponentially with  $N$  in the EFRBN and the SFRBN with  $\langle k \rangle = 2; 4$ , where the function forms of the distributions are almost exponential.

From our results we conclude that a transition occurs near  $\langle k \rangle \sim 2$  in the SFRBN. The result is consistent with that in the "annealed" SFRBN.

In this paper we dealt with the directed graphs that correspond to the asymmetric adjacency matrices in the network theory. However, the quite different distribu-

tions of the state cycle lengths are observed in the undirected random networks. Therefore, it is also interesting to study the properties of the distributions of the state cycle lengths in the undirected scale-free networks as well. The details will be given elsewhere [65].

We have numerically investigated the finite-size networks ( $N = 140 - 1024$ ). In fact, it is very difficult to study the indefinitely large size of systems. This seems the disadvantage of our approach of the finite size systems. However, practically speaking, there are a lot of scale-free-type biological networks with size  $N \sim 10^2 - 10^3$ , such as the metabolic reaction networks of the bacterium *E. coli* and of the Yeast protein interaction networks, etc [47, 66]. Thus, we believe that our results stemmed from the finite size systems might play an important role to study such real network systems in Nature. As we mentioned in the introduction, the asynchronous updating rules are more plausible for biological phenomena. It is interesting to expand the investigation to the asynchronous version.

#### Acknowledgments

We would like to thank Dr. Jun Hidaka for collecting many relevant papers on the Kauffman model and the related topics. One of us (K.I.) would like to thank Kazuko Iguchi for her continuous financial support and encouragement.

#### APPENDIX A: A CASE WITH $h_{ci} = 1$

In this appendix, we compare the numerical results in SFRBN with  $h_{ci} = 1$  with analytical result in RBN with  $K = 1$ .

In Fig. 7, we show the finite-size effect of the mean value  $h_{ci}$ . The analytical result  $h_{ci} = 1.44$  in RBN with  $K = 1$  have been derived based on the probability for distribution of information conserving loops by Flyvbjerg and Kjaer [30]. It is found that the numerical results converge a value 1.44 as the system size increases in both SFRBN and exponential-actuation network.

As mentioned in Sect. IV, we constructed the distribution of the attractor length by different networks with  $h_{ci} = 1$ , i.e. case (A) in introduction. Then the states converge into a point attractor with period unity,  $\tau_c = 1$ , through the transient states in a lot of the network samples. We can partially see the result in the distribution in 2. Accordingly the median  $m$  over the distribution is always unity independent of system size  $N$  in our case.

#### APPENDIX B: DERRIDA PLOTS

In this appendix, we give the numerical results of Derrida plot in the SFRBN. The Derrida plot, analogous

to the Lyapunov exponent in the continuous dynamics,

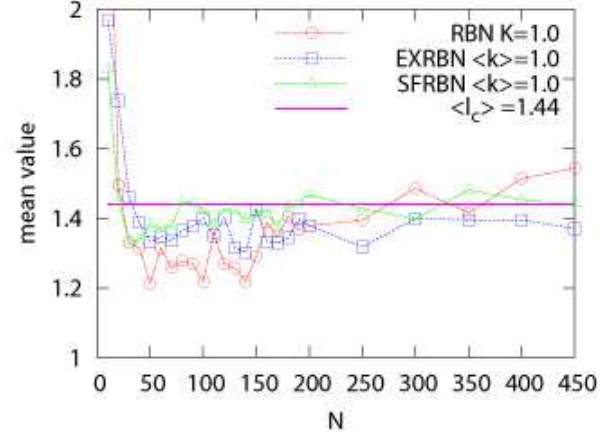


FIG. 7: (Color online) Mean value  $h_{ci}$  of attractor lengths in RBN and SFRBN with  $h_{ci} = 1$ . The analytical result  $h_{ci} = (1 - \log(1 - \tau_c)) / \tau_c = 1.44$  for  $\tau_c = 1/2$  in the annealed RBN is also overplotted.

$m$  measures the divergence of trajectory based on the normalized Hamming distance between two distinct states  $x_i^1(t); x_i^2(t); i = 1; 2; \dots; N$ ,

$$H(t) = \frac{1}{N} \sum_{i=1}^N |x_i^1(t) - x_i^2(t)| \quad (B1)$$

For a sample of the random initial states pairs, the average  $H(t+1)$  is plotted against  $H(t)$ , and the plot is repeated for increasing  $H(t)$ . A curve above the main diagonal  $H(t+1) = H(t)$  indicates a divergent trajectory and chaotic. The area below the diagonal  $H(t+1) = H(t)$  is called the ordered region, because the trajectories converge in the state space. A curve tangential to the main diagonal  $H(t+1) = H(t)$  indicates a critical dynamics.

Figure 8 shows the Derrida plots corresponding to the SFRBN with  $h_{ci} = 1; 2; 4$ . It is apparent that the SFRBN with large  $h_{ci}$  exhibits more chaotic behavior than that with small  $h_{ci}$ . It is important to note that the SFRBN is more ordered than the RBN compared with the cases with  $K = h_{ci}$ . The Derrida coefficient is defined by  $D_c = \log s$ , where  $s$  is the slope of the Derrida plot (curve) at the origin. If  $s = 1$  then  $D_c = 0$ , giving the critical evolution. The slope of the Derrida plot for the SFRBN with  $h_{ci} = 1$  is approximately unity. The result is consistent with the occurrence of the transition at  $h_{ci} = 2$  in the function form of  $m(N)$  observed in Subsec. IV D.

The other quantities such as, the density of frozen nodes and the robustness against perturbation, are also important indicators for the dynamical behavior in the RBN and the SFRBN.



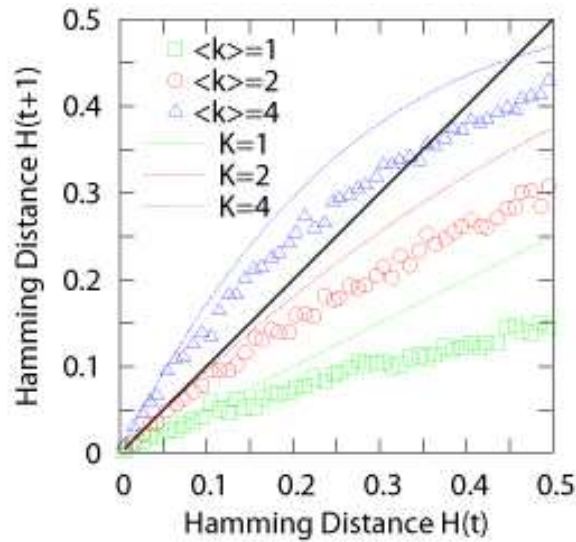


FIG. 8: (Color online) Derrida plots of the SFRBN with  $h_{ki} = 1$ ,  $h_{ki} = 2$  and  $h_{ki} = 4$ . The analytical curves for the RBN with  $K = 1$ ,  $K = 2$  and  $K = 4$  are also overplotted. A line  $H(t+1) = H(t)$  is the dividing line between order and chaos. It is clear that  $K = 2$  lies directly on this line, the system size is  $N = 1024$  and the number of the initial states for averaging is 2000.

- 
- [1] J. Maynard Smith, What Remains To Be Discovered: mapping the species of the universe, the origins of life and the future of the human race, (Touchstone, NY, 1998).
  - [2] M. Eigen, *Naturewissenschaften* 58, 465-523 (1971).
  - [3] S. A. Kauffman, *The Origins of Order: Self-Organization and Selection in Evolution* (Oxford University Press, New York, 1993) and references therein.
  - [4] P. Erdos and A. Renyi, *Publ. Math.* 6, 290 (1959).
  - [5] P. Erdos and A. Renyi, *Publ. Math. Inst. Hung. Acad. Sci.* 5, 17 (1960).
  - [6] P. Erdos and A. Renyi, *Acta Math. Acad. Sci. Hung.* 12 261 (1961).
  - [7] S. A. Kauffman, *J. Theor. Biol.* 22, 437-467 (1969).
  - [8] S. A. Kauffman, *Physica 10D*, 145-156 (1984).
  - [9] B. K. Sawhill and S. A. Kauffman, Working paper, Santa Fe Institute (1997).
  - [10] S. A. Kauffman, *Intern. J. Astrobiol.* 2, 131-139 (2003).
  - [11] S. A. Kauffman, *J. Theor. Biol.* 230, 581-590 (2004).
  - [12] J. E. S. Socolar and S. A. Kauffman, *Phys. Rev. Lett.* 90, 068702 (2003).
  - [13] S. A. Kauffman, C. Peterson, B. Samuelsson, and C. Troein, *Proc. Natl. Acad. Sci. USA* 100, 14796-14799 (2003).
  - [14] B. Derrida and Y. Pomeau, *EuroPhys. Lett.* 1, 45-49 (1986).
  - [15] B. Derrida and G. W. Weisbuch, *J. Physique* 47, 1297-1303 (1986).
  - [16] B. Derrida and D. Stauffer, *EuroPhys. Lett.* 2, 739-745 (1986).
  - [17] H. Flyvbjerg and B. Lautrup, *Phys. Rev. A* 46, 6714-6723 (1992).
  - [18] L. Altenberg, NK Fitness Landscape, Section B2.7.2, in *The Handbook of Evolutionary Computation*, ed. T. Back, D. Fogel, Z. Michalewicz, (Oxford University Press, New York, 1997).
  - [19] M. Adana, S. Coppersmith and L. P. Kadanoff, *Boolean dynamics with Random Couplings*, *nonlin AO*/0204062 (2002).
  - [20] J. Hopfield, *Proc. Natl. Acad. Sci. USA* 79, 2554-2558 (1982); J. Hertz, A. Krogh and R. G. Palmer, *Introduction to the theory of neural computation*, (Perseus Books Publishing, 1991).
  - [21] P. W. Anderson, *Proc. Natl. Acad. Sci. USA* 80, 3386-3390 (1983).
  - [22] D. L. Stein and P. W. Anderson, *Proc. Natl. Acad. Sci. USA* 81, 1751-1753 (1984).
  - [23] P. W. Anderson, *Spin Glass Hamiltonians: A Bridge Between Biology, Statistical Mechanics and Computer Science*, in *Emerging Syntheses in Science*, *Proc. Founding Workshops of the Santa Fe Institute*, ed. D. Pines, (Santa Fe Institute, Santa Fe, 1987), pp.17-20.
  - [24] B. Derrida and H. Flyvbjerg, *J. Phys. A: Math. Gen.* 19, L1003-L1008 (1986).
  - [25] B. Derrida and H. Flyvbjerg, *J. Phys. A: Math. Gen.* 20, 5273-5288 (1987).
  - [26] B. Derrida and H. Flyvbjerg, *J. Physique* 48, 971-978 (1987).
  - [27] B. Derrida and H. Flyvbjerg, *J. Phys. A: Math. Gen.* 20, L1107-L1112 (1987).
  - [28] B. Derrida, *Phil. Mag. B* 56, 917-923 (1987).
  - [29] H. Flyvbjerg, *J. Phys. A: Math. Gen.* 21, L955-L960 (1988).

- [30] H. Flyvbjerg and N. J. Kirk, *J. Phys. A: Math. Gen.* 21, 1695-1718 (1988).
- [31] B. Samuelsson and C. Troein, *Phys. Rev. E* 72, 046112 (2005).
- [32] B. Drossel, T. Mihaljev, and F. Greil, *Phys. Rev. Lett.* 94, 088701 (2005).
- [33] A. Bhattacharyya and S. Liang, *Phys. Rev. Lett.* 77, 1644-1647 (1996).
- [34] U. Bastolla and G. Parisi, *Physica D* 98, 1-25 (1996).
- [35] U. Bastolla and G. Parisi, *J. Theor. Biol.* 187, 117-133 (1997).
- [36] U. Bastolla and G. Parisi, *Physica D* 115, 203-218 (1998).
- [37] U. Bastolla and G. Parisi, *Physica D* 115, 219-233 (1998).
- [38] R. Albert and A.-L. Barabasi, *Phys. Rev. Lett.* 84, 5660-5663 (2000).
- [39] J. E. Socolar and S. A. Kumaran, *Phys. Rev. Lett.* 90, 068702 (2003).
- [40] B. Samuelsson and C. Troein, *Phys. Rev. Lett.* 90, 098701 (2003).
- [41] K. Klumpp and S. Bomholdt, *Phys. Rev. E* 72, 055101 (2005).
- [42] S. N. Coppersmith, L. P. Kadano, and Z. Zhang, *Physica D* 149, 11-29 (2001).
- [43] S. N. Coppersmith, L. P. Kadano, and Z. Zhang, *Physica D* 157, 54-74 (2001).
- [44] S. H. Strogatz, *Nature* 410, 268-276 (2001).
- [45] A.-L. Barabasi, *Linked*, (Penguin books, London, 2002)
- [46] R. Albert and A.-L. Barabasi, *Rev. Mod. Phys.* 74, 47-97 (2002), and references therein.
- [47] A.-L. Barabasi and Z. N. Oltvai, *Nature Reviews* 5, 101 (2004).
- [48] P. Sen et al., *Phys. Rev. E* 67, 036106 (2003).
- [49] G. Wilk, Z. Włodarczyk, *Acta Phys. Polon. B* 36 (2005) 2513-2522. cond-mat/0504253.
- [50] A.-L. Barabasi and E. Bonabeau, *Scientific American* (May), 60-69 (2003).
- [51] M. E. J. Newman, *SIAM Rev.* 45, 167-256 (2003) and references therein.
- [52] B. Luque and R. V. Sole, *Phys. Rev. E* 55, 257-260 (1997).
- [53] R. Albert and A.-L. Barabasi, *Phys. Rev. Lett.* 84, 5660-5663 (2000).
- [54] J. J. Fox and C. C. Hill, *Chaos* 11, 809-815 (2001).
- [55] C. Osawa and A. Savageau, *Physica D* 170, 143-161 (2002).
- [56] X. F. Wang and G.-R. Chen, *IEEE Trans. Circ. Sys.* 49, 54-61 (2002).
- [57] D. Stauffer and A. Aharony, cond-mat/0412612.
- [58] M. Aldana, *Physica D* 185, 45-66 (2003).
- [59] M. Aldana and P. Chuzel, *Proc. Natl. Acad. Sci. USA* 100, 8710-8714 (2003).
- [60] M. Aldana-Gonzalez, S. Coppersmith, and L. P. Kadano, in "Perspectives and Problems in Nonlinear Science", edited by E. K. Aplan, J. E. Marsden, and K. R. Sreenivasan, (Springer-Verlag, NY, 2003), p. 23.
- [61] R. Serra, M. Villani, and L. Agostini, *WIRN VIETRI 2003, LNCS 2859*, (Springer-Verlag, Berlin Heidelberg, 2003), pp. 43-49.
- [62] A. Castro e Silva, J. Kamphorst Leal da Silva, and J. F. F. Mendes, *Phys. Rev. E* 70, 066140 (2004). cond-mat/0410469.
- [63] K. Iguchi, S. Kinoshita, and H. Yamada, *Phys. Rev. E* 72, 061901 (2005). cond-mat/0507055.
- [64] I. Harvey and T. Bossomaier, Time out of joint: Attractors in asynchronous random boolean networks, in *Proceedings of the Fourth European Conference on Artificial Life*, Edited by P. Husbands and I. Harvey, (MIT Press, NY, 1997) pp. 67-75; C. Gershenson, *Artificial Life VIII*, Edited by R. Standish, H. Abbass, M. Bedau, (MIT Press 2002) pp. 1-9.
- [65] S. Kinoshita, K. Iguchi, and H. Yamada, in preparation (2006).
- [66] A. Tang et. al., *Science* 303, 808 (2004).